EBioMedicine 43 (2019) 562–575

Contents lists available at ScienceDirect

EBioMedicine

journal homepage: www.ebiomedicine.com

EBioMedicine
Published by THE LANCET

Research paper

The Notch ligand DNER regulates macrophage IFNγ release in chronic obstructive pulmonary disease

Carolina Ballester-López [a], Thomas M. Conlon [a], Zeynep Ertüz [a], Flavia R. Greiffo [a], Martin Irmler [b], Stijn E. Verleden [c], Johannes Beckers [b,d,e], Isis E. Fernandez [a], Oliver Eickelberg [a,f], Ali Önder Yildirim [a,*]

[a] Comprehensive Pneumology Center (CPC), Institute of Lung Biology and Disease, Helmholtz Zentrum München, Member of the German Center for Lung Research (DZL), Munich, Germany
[b] Institute of Experimental Genetics (IEG), Helmholtz Zentrum München, Munich, Germany
[c] Division of Pneumology, KU Leuven, Leuven 3000, Belgium
[d] Chair of Experimental Genetics, Technische Universität München, Freising, Germany
[e] German Center for Diabetes Research (DZD), Germany
[f] Division of Pulmonary Sciences and Critical Care Medicine, University of Colorado, Denver, CO, USA

ARTICLE INFO

Article history:
Received 11 December 2018
Received in revised form 28 February 2019
Accepted 19 March 2019
Available online 4 May 2019

Keywords:
COPD
Macrophages
DNER
Notch signalling
IFNγ
Cigarette smoke
Lung
NFkB

ABSTRACT

Background: Chronic Obstructive Pulmonary Disease (COPD) is the third leading cause of death worldwide with no curative therapy. A non-canonical Notch ligand, DNER, has been recently identified in GWAS to associate with COPD severity, but its function and contribution to COPD is unknown.
Methods: DNER localisation was assessed in lung tissue from healthy and COPD patients, and cigarette smoke (CS) exposed mice. Microarray analysis was performed on WT and DNER deficient M1 and M2 bone marrow-derived macrophages (BMDM), and gene set enrichment undertaken. WT and DNER deficient mice were exposed to CS or filtered air for 3 day and 2 months to assess IFNγ-expressing macrophages and emphysema development. Notch and NFKB active subunits were quantified in WT and DNER deficient LPS-treated and untreated BMDM.
Findings: Immunofluorescence staining revealed DNER localised to macrophages in lung tissue from COPD patients and mice. Human and murine macrophages showed enhanced DNER expression in response to inflammation. Interestingly, pro-inflammatory DNER deficient BMDMs exhibited impaired NICD1/NFKB dependent IFNγ signalling and reduced nuclear NICD1/NFKB translocation. Furthermore, decreased IFNγ production and Notch1 activation in recruited macrophages from CS exposed DNER deficient mice were observed, protecting against emphysema and lung dysfunction.
Interpretation: DNER is a novel protein induced in COPD patients and 6 months CS-exposed mice that regulates IFNγ secretion via non-canonical Notch in pro-inflammatory recruited macrophages. These results provide a new pathway involved in COPD immunity that could contribute to the discovery of innovative therapeutic targets.
Funding: This work was supported from the Helmholtz Alliance 'Aging and Metabolic Programming, AMPro'.

1. Introduction

COPD is currently the third leading cause of death worldwide with 10% of people past forty affected [1,2]. Exposure to environmental particles, especially cigarette smoke, is the most common cause of COPD. These patients exhibit a progressive airflow obstruction provoked by small airway fibrosis, alveolar wall destruction (emphysema) and chronic inflammation [3]. In the last decades, it has become evident that inflammatory cells play a key role in initiating and perpetuating the disease pathology [4–9]. Firstly, inflammation is rapidly recognizable by an increase of neutrophils and macrophages in the lung. Indeed, macrophage-driven inflammation is one of the main triggers driving an abnormal immune response. It is believed that most of these macrophages are derived from bone marrow-derived blood monocytes that have been quickly recruited to the site of injury rather than expansion of lung tissue resident macrophages [10]. In a disease context, macrophages can acquire distinct phenotypes attending to the local microenvironmental needs. It is generally accepted the existence of two main phenotypes: activated (M1) and alternative (M2) macrophages,

* Corresponding author at: Comprehensive Pneumology Center (CPC), Institute of Lung Biology and Disease, Helmholtz Zentrum München, Ingolstädter Landstraße 1, Neuherberg 85764, Germany.
E-mail address: oender.yildirim@helmholtz-muenchen.de (A.Ö. Yildirim).

https://doi.org/10.1016/j.ebiom.2019.03.054

Research in context

Evidence before this study

COPD is a complex and progressive disease whose pathology is mainly driven and perpetuated by chronic inflammation. In fact, current treatments are mainly immunosuppressive drugs in combination with bronchodilators that mitigate the symptoms but do not cease disease progression. Hence, there is an urgent need of finding new molecular targets that can be implicated in disease development. Therefore, we searched for recent GWAS studies with healthy and COPD patients using PubMed and the GWAS central database (search terms: "GWAS COPD" "SNP COPD"). We found DNER as a potential genetic risk confirmed by 2 independent GWAS. Additionally, *DNER* gene expression was upregulated in smoker patients analysed in the GWAS studies. However, we could not find any study addressing DNER lung cell localisation and function (sources: Pubmed, UniProt, NextBio). Thus, our aim was to unravel how DNER is implicated in COPD development.

Added value of this study

Here we showed that DNER is expressed in pro-inflammatory recruited alveolar macrophages where it regulates IFNγ release during chronic inflammation in a CS-induced COPD mouse model. Furthermore, we provided the first evidence of DNER as a regulator of Notch1-NFKB crosstalk in activated macrophages.

Implications of all the available evidence

Today there are few studies dedicated to following up new gene candidates obtained from GWAS, usually due to the considerable lack of knowledge about these novel proteins. DNER is a protein well described in the nervous system but no detailed research has been investigated in other organs or cell types. This is the first study showing a functional role and molecular mechanism for DNER in lung macrophages, regulating IFNγ release. Moreover, the controversial and little understanding of the non-canonical Notch pathway entails an additional novel angle to our research, since the molecular mechanism of DNER published in neurons was not observed in macrophages. Lastly, it is known that cigarette smoke IFNγ-driven inflammation is the main trigger of COPD immunopathology, mostly released by macrophages and Th1 cells. Here we showed that DNER regulates IFNγ expression in macrophages during CS-induced chronic inflammation. Taken altogether, our study offers new molecular and functional knowledge on DNER and non-canonical Notch signalling as well as contributes to enlightening novel therapeutic strategies for COPD patients.

originally defined based on in vitro settings [11]. M1 are responsive to type 1-driven inflammation by secreting inflammatory cytokines like IL-12a or TNFα, while M2 are induced by type 2 stimulation and are involved in tissue remodelling, anti-inflammatory response and efferocytosis [12]. During COPD, the altered biology of the lung together with the pleiotropic effects and plasticity of macrophages, results in a continuous phenotype shifting that makes it difficult to discriminate M1 and M2 [13]. Indeed, it has been postulated the existence of at least 8 different phenotypes [10]. However, it is known in COPD that M1 and M2 subpopulations are defective in their ability to respond to the environment although it is not clear if there is a dominant phenotype [14,15]. Nevertheless, as the disease progresses, dysfunctional macrophages lead to an exacerbated and inefficient inflammatory response contributing to tissue damage and enhanced susceptibility to bacterial and virus infections [14,16]. Macrophage responses are thus precisely controlled by a wide range of cellular pathways [17], among them Notch signalling [18], although further investigation is needed to fully understand the molecular mechanisms.

Given the complexity and heterogeneity of COPD pathology, there is an unmet therapeutic need since current treatments only alleviate the symptoms but do not interrupt or reverse disease progression [1]. This lack of a curative therapy leads to the necessity of searching new targets. Hancock and colleagues in 2012 identified a SNP located in the intronic region of *DNER* (Delta Notch like epidermal growth factor related receptor), as the most significant SNP associated with the FEV1/FVC ratio and FEV1 [19]. Indeed, a further GWAS using an expanded cohort (16,707 subjects) confirmed the relevance of this SNP as a genetic risk for COPD and pulmonary function [20].

DNER is a transmembrane protein that belongs to the non-canonical Notch ligand family and binds to the Notch1 receptor [21,22]. In contrast to canonical, the non-canonical pathway is triggered by a different family of ligands that differ in their protein structure and whose downstream cascade leads to CSL (CBF1, Suppressor of Hairless, Lag-1) independent Notch activation. DNER was first described to be highly expressed by Purkinje neurons where it played a key role in cerebellum development [23,24], but it is also involved in differentiation and proliferation during cancer and stemness [25,26]. Nevertheless, its function in other cell types or in lung disease is completely unknown. Moreover, implication of the non-canonical Notch pathway in the immunopathogenesis of COPD has never been elucidated. Therefore, we hypothesize that the non-canonical Notch ligand DNER contributes to the promotion of pro-inflammatory responses during the progression of COPD pathogenesis.

Here, we demonstrate that DNER is expressed and localised to macrophages of experimental and human COPD. Furthermore, we provided evidence ex vivo and during disease pathogenesis that downstream DNER signalling is crucially involved in IFNγ secretion by pro-inflammatory murine macrophages via activation of Notch1-NFκB crosstalk. Collectively, this study is the first to describe the function and mechanism of DNER in macrophages in the context of chronic lung inflammation and opens new avenues to discover novel therapeutic targets for COPD patients.

2. Material and methods

2.1. Human tissue samples

Lung core samples from COPD patients (Supplementary Table 1) prior to lung transplantation were provided by Dr. Stijn Verleden (University of Leuven, Belgium), following ethical approval of the University of Leuven Institutional Review Board (S52174). All participants gave written consent and experiments were carried out following the principles described in the Declaration of Helsinki. COPD patients were explanted between 2009 and 2015. Controls were obtained from lungs not suitable for transplantation due to different reasons (kidney tumor, logistics, presence of microthrombi). Lung conditions were evaluated based on stereology/morphology parameters and CT. According to Belgian law, declined donor lungs can be designated for research after second opinion examination. Control subjects were explanted between 2011 and 2018. After organ removal, lungs were air-inflated at 10 cm H_2O pressure and fixed with liquid nitrogen vapour. Lungs were then cut into pieces with a band saw and sampled with a core bore. For paraffin embedding, lung pieces were sliced and fixed in 4% paraformaldehyde. For isolation of total RNA (peqGOLD Total RNA Kit, Peqlab), lung cores were snap frozen in liquid nitrogen.

2.2. Human monocyte derived macrophages

Human macrophages were differentiated from PBMCs of four healthy donors. Informed written consent was provided by all

participants and the local ethical review board approved the use of human tissue (180–14 LMU board). Briefly, 5×10^6 PBMCs were cultured in amino acids, 1 mM sodium pyruvic acid, 9 mg of bovine insulin (Sigma Chemical Co., St Louis, Mo) and the presence of 100 ng/ml M-CSF for 7 days. After differentiation, macrophages were treated for 24 h with 1 μg/ml LPS (*E. coli* O55:B5, Sigma-Aldrich) and 5% cigarette smoke extract (CSE).

2.3. Mice

C57BL/6 N *Dner*$^{tm3b(EUCOMM)Hmgu}$ (*Dner*$^{-/-}$) mice were obtained from the German Mouse Clinic (GMC), Helmholtz Zentrum München. Mice were allowed food and water ad libitum, kept at a constant temperature and humidity, with a 12-h light cycle, under specific pathogen free conditions. All animal experiments were performed following strict governmental and international guidelines and were approved by the local government for the administrative region of Upper Bavaria, Germany.

2.4. Cigarette smoke exposure

8–12 weeks old C57BL/6 N and *Dner*$^{-/-}$ mice were exposed to 100% mainstream of 500 mg/m^3 cigarette smoke (CS) [57], using 3R4F research cigarettes (Filter removed, Tobacco Research Institute, University of Kentucky), for 50 min twice/day, for 3 days, and 5 days/week for 2 months or 6 months. Mice exposed to filtered air were used as controls.

2.5. Lung function test

Lung function analysis was performed as previously described [4]. In summary, anaesthetised mice were tracheostomized and cannulated before the test. Respiratory function (forced expiratory volume after 100 ms, FEV100) was analysed using a forced pulmonary maneuver system [5] (Buxco Research Company, Data Sciences International) running FinePointe Software (version 6, Data Sciences International) and the quasistatic PV maneuver protocol.

2.6. Bronchoalveolar lavage (BAL)

Lungs were washed three times with 500 μl of sterile PBS (Gibco, Life Technologies) supplemented with Complete Protease Inhibitor Cocktail tablets (Roche Diagnostics). BAL cells were pelleted and resuspended in 500 μl RPMI-1640 medium (Gibco, Life Technologies) for the total cell count. Cytospins of the cell suspensions were prepared and stored at −80 °C for immunofluorescence staining.

2.7. Mouse lung processing

The two right lower lung lobes were stored in liquid nitrogen for RNA and protein isolation. The right upper two lobes were dissociated into single cell suspensions in MACS buffer using the lung dissociation kit and gentleMACS Dissociator (Miltenyi Biotec) for flow cytometry analysis. The left lung was fixed with 6% paraformaldehyde under a pressure of 20 cm inflation and paraffin embedded.

2.8. Flow cytometry

10^6 cells from filtered single cell lung homogenates or BAL cell pellets were blocked with purified anti-mouse CD16/CD32 (Clone: 93, eBioscience) for 20 min followed by 30 min incubation with antibody cocktails on ice. For intracellular staining, cells were fixed with 4% PFA for 10 min and then permeabilized with 1% BSA/0.5% Saponin/PBS buffer followed by 10 min incubation with anti-mouse CD16/CD32 and a second incubation of antibody cocktails in the permeabilization buffer. After washing and re-suspending in MACS buffer (Miltenyi Biotec), cells were analysed on a BD FACSCanto II flow cytometer (BD Biosciences) running BD FACSDiva software. B cell and T cell staining was performed with: APC-conjugated anti-CD19 (clone: 6D5, Miltenyi Biotec), APC-Vio770-conjugated anti-CD3e (clone: 17A2, Miltenyi Biotec), PE-Vio770-conjugated anti-CD22 (clone: Cy34.1, Miltenyi Biotec), PE-conjugated anti-CD80 (clone: 16-10A1, Miltenyi Biotec), PerCP-Vio700-conjugated anti-MHCII (clone: M5/114.15.2, Miltenyi Biotec), VioGreen-conjugated anti-CD69 (clone: H1.2F3, Miltenyi Biotec), FITC-conjugated anti-IgG (Biolegend). For the macrophage profile: VioGreen-conjugated anti-CD45 (clone: 30F11, Miltenyi Biotec), APC-Vio770-conjugated anti-Ly6C (clone: 1G7.G10, Miltenyi Biotec), VioBlue-conjugated anti-Ly6G (clone: 1A8, Miltenyi Biotec), FITC-conjugated anti-MHCII (clone: M5/114.15.2, Miltenyi Biotec), PerCP-Vio700-conjugated anti-F4/80 (clone: REA126, Miltenyi Biotec), PE-Vio770 conjugated anti-Siglec-F (clone: ES22-10D8, Milteyi Biotec), PE-conjugated anti-CD11b (clone: M1/70.15.11.5, Miltenyi Biotec), APC-conjugated anti-CD11c (clone: N418, Miltenyi Biotec). For intracellular staining: APC conjugated anti-IL-4 (clone: 11B11, BIOZOL Diagnostica) and FITC conjugated anti-IFNγ (clone: XMG1.2, Life Technologies).

2.9. Immunofluorescence

3 μm murine or human lung tissue sections were deparaffinized and rehydrated followed by heat-induced epitope retrieval using HIER Citrate Buffer (pH 6.0, Zytomed Systems). For the cytospins, cells were fixed by incubation with methanol for 10 min followed by 1 min of acetone. Sections or cytospins were blocked with 5% BSA for 30 min, incubated overnight at 4 °C with primary antibodies and 1 h at room temperature with secondary antibodies (anti-goat Alexa Fluor 568, anti-rabbit Alexa Fluor 488, anti-mouse Alexa Fluor 488 and anti-rabbit Alexa Fluor 555, Life Technologies) diluted in 1% BSA. Images at different magnifications were captured using Axio Imager with an M2 microscope (Zeiss) and processed with ImageJ 1.x [58]. Primary antibodies common for human and murine tissue: Galectin-3 (1:50 sc-32790, Santa Cruz), CD31 (1:50 ab28364, Abcam), ACTA-2 (1:600 ab5694, Abcam), Pro-SPC (1:100 AB3786, Chemicon International). Human tissue: DNER (1:100 AF3646, R&D Systems), CC10 (1:100 sc-365992), NOS2 (1:20 sc-8310). Murine tissue: DNER (1:50 AF2254, R&D Systems), NICD1 (1:25 ab8925, Abcam).

2.10. Quantitative morphometry

Design-based stereology was used to analyse mean chord length in H&E stained tissue sections using the new Computer Assisted Stereological Toolbox (newCAST, Visiopharm) and an Olympus BX51 light microscope as described [5]. In brief, 20 frames were randomly selected by the software across multiple sections under the x20 objective and superimposed by a line grid and points. The intercepts of lines with alveolar wall (I_{septa}) and points localised on air space (P_{air}) were counted and calculated as $MCL = \sum P_{air} \times L(p) / \sum I_{septa} \times 0.5$, where L(p) is the line length per point.

2.11. Professional APC isolation and stimulation

Bone marrow was flushed from femurs and tibias of C57BL/6 N and *Dner*$^{-/-}$ mice with RPMI-1640 medium. Bone marrow cells were passed through 40 μm filters (Miltenyi Biotec), counted and resuspended in 5% fetal bovine serum, 50 μM β-mercaptoethanol and 100 U/ml penicillin and streptomycin RPMI-1640 medium. 2×10^6 cells/ml were plated in T25 Flasks for protein isolation and nuclear extractions or in 24 well plates for RNA isolation. Medium was additionally supplemented with 20 ng/ml of murine recombinant M-CSF to generate bone marrow derived macrophages (BMDM) or 20 ng/ml murine recombinant GM-CSF for bone marrow derived dendritic cells (BMDC). Medium was changed every 2–3 days carefully discarding non-

adherent cells. For BMDM, on day 7 fresh medium without M-CSF was added and left overnight. For BMDCs, on day 7 to 8 adherent cells were harvested and 1×10^7 cells were seeded in 100 mm petri dishes to keep them in culture for an additional 24-48 h. The non-adherent maturing DCs were collected as they were released. BMDM were stimulated with 1 μg/ml LPS (from E.coli 0111:B4, Sigma-Aldrich) and 20 ng/ml of recombinant murine IFNγ (M1 phenotype) or with 20 ng/ml of recombinant murine IL-4 (M2 phenotype) for 24 h. BMDCs were treated with 1 μg/ml LPS for 24 h. All cytokines were purchased from ImmunoTools.

2.12. Th differentiation

Naive CD4 T cells were purified from total murine splenocytes using the $CD4^+$ $CD62L^+$ T cell Isolation Kit II (Miltenyi Biotec) and cultured at 1.5×10^6/ml in RPMI1640 medium supplemented with 10%FCS, 0.1 mM beta-mercaptoethanol, 100 U/ml penicillin Streptomycin, 10 mM HEPES, 1 mM Sodium Pyruvate, 0.1 mM non essential amino acids and 1 × MEM Vitamin Solution. These were then stimulated for 48 h with anti-CD3/anti-CD28 coupled beads, along with recombinant human TGFβ (10 ng/ml, R&D Systems, Wiesbaden, Germany), IL-6 (60 ng/ml, R&D Systems), anti-IL-4 (10 μg/ml, BioLegend, San Diego, CA), anti-IL-12 (10 μg/ml, BioLegend), anti-IFNγ (5 μg/ml, BioLegend) and anti-IL-2 (2.5 μg/ml, Miltenyi Biotec) for Th17 differentiation. For Th2, anti-CD3/anti-CD28 coupled beads were supplemented with recombinant mouse IL-4 (20 ng/ml, R&D systems, anti-IL12 (10 μg/ml) and anti-IFNgamma (5 μg/ml) for 96 h. For Th1, with recombinant IL-12p70 (10 ng/ml, BD Pharmingen) and anti-IL-4 (10 μg/ml) for 96 h. For Treg differentiation anti-CD3/anti-CD28 coupled beads were supplemented with recombinant human TGFβ (10 ng/ml, R&D Systems) and 1000 IE/ml recombinant human IL-2 (ProleukinS, Novartis) for 72 h. Th0 control cells were stimulated with anti-CD3/anti-CD28 coupled beads alone for a comparable period of time. For Th1 and Th2 differentiation and their Th0 control, the culture volume was doubled with medium containing 1000 IE/ml recombinant human IL-2 at 40 h and at 80 h the medium was replaced with medium lacking IL-2.

2.13. Cell lysates

To obtain whole cell lysates, BMDM were washed with ice-cold PBS and collected by scraping into RIPA buffer. Samples were incubated for 30 min on ice mixing every 5 min. Lysates were centrifuged at 13000 rpm for 15 min at 4 °C and supernatants retained. To perform cytoplasmic and nuclear extractions from BMDM, a commercial kit was used and undertaken as per manufacturers instructions (Nuclear Extract Kit 40010 and 40410, Active Motif).

2.14. Western blotting

20 μg of cell lysates were diluted in Laemmli Buffer (BioRad) containing β-mercaptoethanol (Gibco, Life Technologies) and incubated for 10 min at 95 °C. Protein samples were separated on a 10% sodium dodecyl sulfate–polyacrylamide gel by electrophoresis and wet-transferred to a PVDF membrane (BioRad). Membranes were blocked with Roti buffer (Roti®-Block protein free, Roth) for 1 h, then incubated with primary antibody overnight at 4 °C followed by 1 h incubation with secondary antibody at room temperature. Primary antibodies: NICD1 (1:500, ab8925, Abcam), RelB (1:200, sc-226, Santa Cruz), cRel (1:100, sc-6955, Santa Cruz), p105/50 (1:100, sc-1190, Santa Cruz), p65 (1:500, sc-372, Santa Cruz), pIKKα/β (1:1000 #2697, Cell Signalling), IKKα (1:1000 #2682S, Cell Signalling), IKKβ (1:1000 clone D30C6, #8943, Cell Signalling). Secondary antibodies: rabbit anti-goat IgG-HRP (1:5000, 2768 Santa cruz), Anti-rabbit IgG-HRP (1:3000, 7074P2 New England Biolabs), and anti-mouse (1:3000, NA931V GE Healthcare).

2.15. Cigarette smoke extract (CSE) preparation

CSE was prepared as previously described [4]. Briefly, cigarette smoke from 3 cigarettes (3R4F, Tobacco Research Institute, University of Kentucky) was bubbled through 30 ml of cell culture medium at a constant speed, in a closed environment. The resultant solution was considered as 100% CSE.

2.16. ELISA

Total IFNγ cytokine levels were measured in BAL from 3 days and 2 months CS exposed C57BL/6 N and *Dner*$^{-/-}$ mice and in cell supernantants from BMDMs using a commercial kit following the manufacturer's instructions (murine IFNγ PEP-900-K98, Preprotech).

2.17. RNA isolation and quantitative real time RT-PCR and end point PCR

RNA from tissue or cells was isolated as described using the peqGOLD total RNA kit (Peqlab). 0.5-1 μg RNA was reverse transcribed using Random Hexamers and MuLV Reverse Transcriptase (Applied Biosystems). To analyse gene expression, Platinum™ SYBR™ Green qPCR SuperMix-UDG (Thermo Fisher) on a StepOnePlus 96 well Real-Time PCR System (Applied Biosystems) was used. Primer sequences can be found in Supplementary Table 2. Gene relative expression was calculated using *HPRT1* or *Hprt1* as housekeeping genes ($2^{-\Delta Ct}$). For end point PCR, cDNA fragments were amplified in a thermo cycler using Green GoTaq Polymerase (Promega) and separated in a 2% agarose gel. Primer sequence: *Dner* 5′-CAT AAT CCT GCC CCG CTC TC-3′, 3′-TCATTTGAGTGGCTGTCCCC-5′.

2.18. Microarray

Total RNA from C57BL/6 N and *Dner*$^{-/-}$ M0, M1 and M2 BMDM was isolated with peqGOLD total RNA kit (Peqlab) including digestion of remaining genomic DNA. The Agilent 2100 Bioanalyzer was used to assess RNA quality and only high quality RNA (RIN > 7) was used for microarray analysis. For the expression profiling, about 30 ng of RNA was amplified using the Ovation Pico WTA System V2 in combination with the Encore Biotin Module (NuGEN Technologies, Inc., San Carlos, CA, USA). Amplified cDNA was hybridized on a mouse Gene 2.0 ST array (Affymetrix, Santa Clara, CA, USA). Staining and scanning (Scanner 3000 7G) was done according to the Affymetrix expression protocol including minor modifications as suggested in the Encore Biotion protocol (NuGEN Technologies, Inc). Array data has been submitted to GEO (GSE119257).

2.19. Transcriptome analysis

Expression console (v.1.4.1.46, Thermo Fisher Scientific Inc.) was used for quality control and to obtain annotated normalized RMA gene-level data (standard settings including median polish and sketch-quantile normalisation). Statistical analyses were performed by utilizing the statistical programming environment R (R Development Core Team [59]). Genewise testing for differential expression was done employing the (limma) *t*-test ($p < 0.05$) and cut-offs for ratio (>1.3-fold) and expression levels (average > 16 in at least one experimental group per comparison) were applied. PCA was done in R and the upstream regulator analysis was generated through the use of QIAGEN's Ingenuity Pathway Analysis (IPA®, QIAGEN Redwood City, www.qiagen.com/ingenuity).

2.20. Gene set enrichment analysis (GSEA)

Enrichment of defined sets of genes in our microarray data and data obtained from series matrix files downloaded from the NCBI GEO database (GSE8608) was performed using the GSEA software from the

Broad Institute (http://www.gsea-msigdb.org/gsea/index.jsp) [60]. The following molecular signature databases obtained from the GSEA collection were examined; canonical pathways (CP) REACTOME (gene set size filters: 30–500 genes, 270 gene sets), gene ontology (GO) molecular function (gene set filters: 15–500 genes, 659 gene sets).

2.21. Statistical analysis

No statistical procedure was applied to define the number of samples. GraphPad Prism (Version 6, GraphPad Software) was used for all statistical analysis. Data are presented as mean ± SD with sample size and number of repeats indicated in the Figure legends. For comparison between two groups statistical significance was analysed with Student's *t*-test *p* values <.05 were considered significant. For multiple comparisons, one-way ANOVA (one variable) or two-ways ANOVA (two variables) and Tukey's multiple comparisons test were used ($^{*}P < 0.05$, $^{**}P < 0.01$, $^{***}P < 0.001$, $^{****}P < 0.0001$).

3. Results

3.1. DNER is localised to activated macrophages in COPD patients

To determine the relevance of DNER in COPD evidenced by the GWAS studies [19,20], we assessed *DNER* expression in whole lung homogenates from healthy and COPD patients. *DNER* transcription was significantly increased in COPD patients compared to healthy controls independently of both gender and age (Fig. 1a, Supplemental Fig. 1a-b). In human lung histological sections, DNER co-localised with the macrophage marker Galectin-3 in both healthy and COPD patients (Fig. 1b, Supplemental Fig. 1c), suggesting that macrophages are the predominant DNER-expressing cells. Given the predominance of inflammation in a COPD lung, human monocyte derived macrophages (MDM) were treated with LPS plus cigarette smoke extract (CSE) to mimic the COPD microenvironment in vitro. Interestingly, *DNER* expression was significantly induced as well as the pro-inflammatory marker, *TNF* (Fig. 1c). Supporting this data, DNER co-localised with the pro inflammatory M1 marker NOS2 in human lung tissue (Fig. 1d). These results strongly suggest that pro-inflammatory human macrophages are the main cell type expressing DNER in the human lung and likely harbour DNER function during COPD development.

3.2. DNER is expressed in murine M1 macrophages and regulates IFNγ signalling

The cigarette smoke (CS)-induced COPD mouse model was used to further investigate the role of DNER in the immunopathogenesis of COPD. After 6 months of CS exposure, wild-type (WT) mice develop emphysema, airway remodelling and chronic lung inflammation [4], the main characteristic pathological changes observed in human COPD patients [3,27]. Immunofluorescence staining revealed that DNER localised to macrophages of CS-exposed COPD mice (Fig. 2a), supporting the previous findings in human tissue. As already mentioned, macrophage-driven inflammation in the context of COPD plays an important role in disease onset. Therefore, we next exposed bone marrow derived macrophages (BMDM) from WT mice to pro (M1) or anti- (M2) inflammatory stimuli and assessed *Dner* expression. Validation of BMDM differentiation was confirmed by FACS analysis (90.7% of the obtained population was F4/80^{+} CD11b^{+} CD11c^{-} Ly6g^{-} Ly6c^{-}, Supplementary Fig. 1d). Interestingly, M1 BMDM revealed significantly increased expression of *Dner* (Fig. 2b). In contrast, bone marrow derived DCs (BMDC) treated with LPS did not increase *Dner* levels, suggesting that murine macrophages are the only antigen presenting-cell that express *Dner* in response to inflammation (Supplementary Fig. 1e). To address whether DNER has a role in macrophage polarisation, microarray analysis of WT and DNER deficient BMDM polarised populations was performed. DNER deficient mice were created by deletion of *Dner* exon 3 using the Cre-LoxP system and knock out efficiency was confirmed by the absence of DNER transcript and protein in brain tissue and macrophage lysates from knock out mice (Supplementary Fig. 2a-c). Principal component analysis (PCA) revealed that M0, M1 and M2 populations were similarly clustered for both WT and DNER deficient BMDM, indicating that global macrophage polarisation is not affected by the absence of DNER (Supplementary Fig. 2d). Likewise, M1 (*Tnf*, *il12a*) and M2 (*Fizz1*, *Arg1*) markers exhibited comparable expression levels in both genotypes, confirming similar polarisation (Supplementary Fig. 2e).

Even though DNER did not influence macrophage polarisation, its expression levels are significantly elevated in M1 macrophages (Fig. 2b), which could suggest a role in signalling pathway regulation. To further analyse the downstream cascade of DNER in M1 macrophages, we performed gene set enrichment analysis (GSEA). Investigating a combination of 270 REACTOME pathway gene sets, revealed that interferon signalling was the most enriched pathway in WT M1 compared to DNER deficient M1 BMDM (Fig. 2c, d). Given the diversity and complexity of interferon signalling, we next determined which type of interferon pathway is impaired in DNER deficient mice. Interestingly, induction of type II interferon (*Ifng*), but not type I (*Ifnb1*), was significantly abrogated in M1 polarised DNER deficient compared to WT BMDM (Fig. 2e). Supporting the idea of *Ifng* as a possible downstream target of DNER, IFNγ signalling was found to be enriched in WT M1 (Fig. 2f, Supplementary Fig. 2f). Furthermore, GSEA from an online available dataset of monocyte derived macrophages (MDM) obtained from healthy and COPD patients (GSE8608) [28], revealed an enriched IFNγ pathway in COPD MDM (Fig. 2g). It should be considered that T cells, specifically Th1 cells, serve as a major source of IFNγ. However, in vitro differentiated WT T cell subpopulations showed very low expression of *Dner*, therefore making it unlikely that DNER regulates IFNγ in T cells (Supplementary Fig. 3f). Hence, these data indicated that DNER is significantly enhanced in M1 macrophages where it specifically regulates IFNγ expression.

3.3. DNER regulates IFNγ in recruited macrophages during chronic CS exposure

The persistent inflammation observed in COPD is mainly caused by the continuous secretion of pro-inflammatory cytokines, among them IFNγ is essential to maintain cytokine production and immune cell recruitment and polarisation [29]. To investigate whether in vivo DNER deficiency affects the release of IFNγ during acute and chronic inflammation, WT and DNER deficient mice were exposed to CS for 3 days (acute) or 2 months (chronic) (Supplementary Fig. 3a). Immunofluorescence staining of the bronchoalveolar lavage (BAL) macrophages from 3 days and 2 months of CS exposure revealed increased DNER expression in macrophages compared to filtered air treated animals (Fig. 3a), confirming that DNER expression is triggered in pro-inflammatory macrophages (M1). Similarly, in BAL fluid from 2 month CS-exposed mice, IFNγ levels were significantly induced in WT mice but this was not significantly enhanced in DNER deficient animals (Fig. 3b). To clarify whether DNER regulates macrophage IFNγ secretion during chronic inflammation, we analysed the lung macrophage population from chronic CS-exposed mice by flow cytometry. In line with the in vitro results, CD45^{+} Ly6g^{-} F4/80^{+} alveolar macrophages from WT mice exhibited significant IFNγ induction after chronic CS exposure which was diminished in DNER deficient mice (Fig. 3c).

To elucidate whether recruited or resident macrophages differentially secrete IFNγ in the absence of DNER, we analysed both populations by gating on CD45^{+}Ly6g^{-} F4/80^{+} SiglecF^{-} (recruited) or CD45^{+}Ly6g^{-} F4/80^{+}SiglecF^{+} (resident) populations (Fig. 3d). Strikingly, recruited macrophages from DNER deficient mice were unable to secrete IFNγ in response to CS exposure, as determined by both the percentage of IFNγ positive cells and the mean fluorescence intensity (MFI) (Fig. 3e). In contrast, resident macrophages did not show any

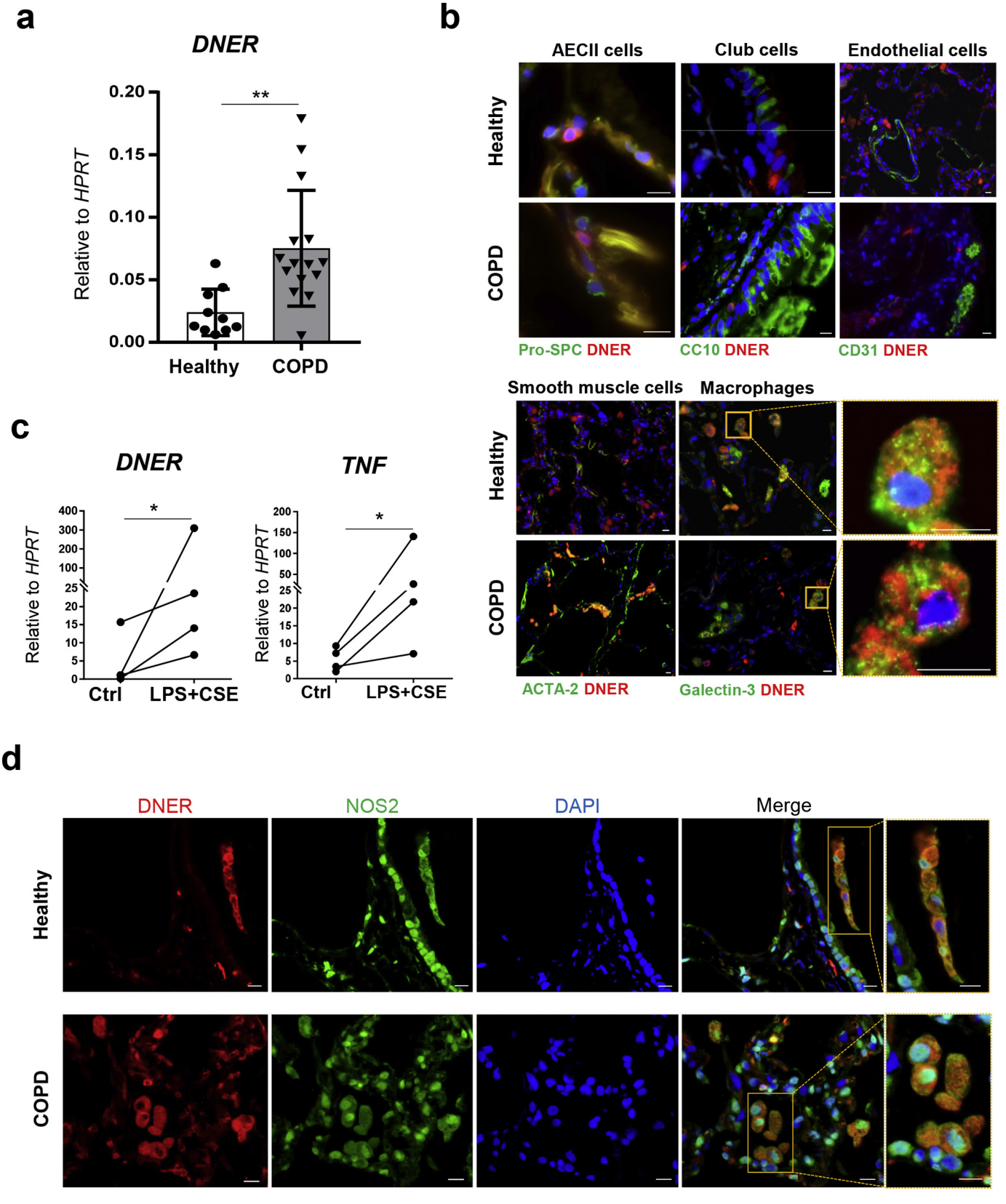

Fig. 1. *DNER* is significantly upregulated in lung tissue from COPD patients and localised to pro-inflammatory macrophages. (a) *DNER* mRNA abundance in lung tissue from healthy subjects ($n = 10$) and COPD patients ($n = 15$). $^{**}p$-value = 0.003, unpaired *t*-test. Data shown mean values ± SD. (b) Representative immmunofluorescence images from healthy and COPD lung tissue ($n = 2/3$) stained to detect localisation of DNER (red), DAPI (blue) and Pro-SPC/CC10/CD31/Acta2/Galectin-3 (green). Scale bar, 10 μm. (c) *DNER* and *TNF* mRNA abundance in human monocyte derived macrophages obtained from PBMCs of healthy subjects ($n = 4$) and treated with 1 μg/ml LPS in combination with cigarette smoke extract (CSE) 5% for 24 h. Paired *t*-test, $^{*}p = 0.0408$. (d) Representative immunofluorescence pictures of DAPI (blue), NOS2 (green) and DNER (red) staining in healthy and COPD lung tissue ($n = 3$). Scale bar, 10 μm.

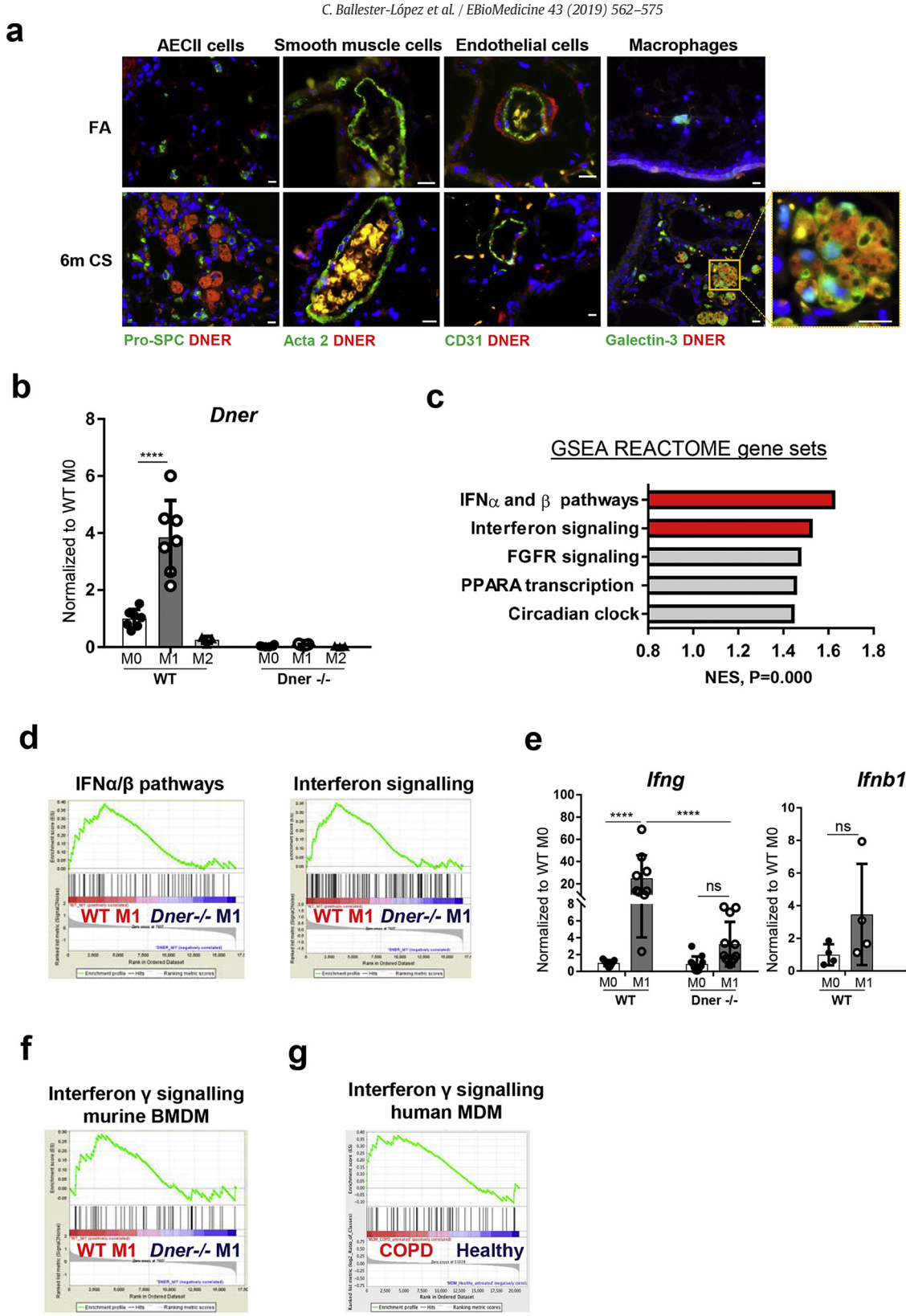

Fig. 2. DNER is localised to macrophages in 6 m CS-exposed mice and regulates IFNγ response in M1 BMDM. (a) Representative immmunofluorescence images of lung tissue from filtered air (FA) and 6 month CS-exposed mice stained with DNER (Red), DAPI (Blue) and Galectin-3/Pro-SPC/Acta-2/CD31 (green) (n = 2–3 mice per group). Scale bar, 10 μm. (b) *Dner* mRNA levels in WT and DNER deficient bone marrow derived macrophages (BMDM) treated with 1 μg/ml LPS and 20 ng/ml IFNγ (M1) or 20 ng/ml IL-4 (M2) or untreated (M0). (c) Top 5 pathways with the highest Normalized Enriched Scores (NES) in Gene set enrichment analysis (GSEA) of the microarray data from WT M1 vs DNER deficient M1 BMDM using a list of 270 REACTOME pathway gene sets obtained from the Broad Institute software. (d) Enrichment plots from (2c) of WT M1 vs DNER deficient M1 BMDM. (e) mRNA levels of *Ifnb1* and *Ifng* in M0 and M1 BMDM populations. (f) Enrichment plot of IFNγ signalling following GSEA analysis of the microarray data from WT M1 vs DNER deficient M1 BMDM. (g) Enrichment plot of IFNγ signalling from the GSEA analysis of Monocyte Derived Macrophages (MDM) obtained from healthy and COPD patient microarray data (NCBI GEO dataset, GSE8608). Two-way ANOVA, Tukey's multiple comparisons test, $^{****}P < 0.0001$ (b, e). Representative 2 independent experiments out of 5, $n = 3$ mice, 2–3 replicates per mouse (b, e). One experiment, $n = 3$ (c-d, f-g). Data shown mean values ± SD.

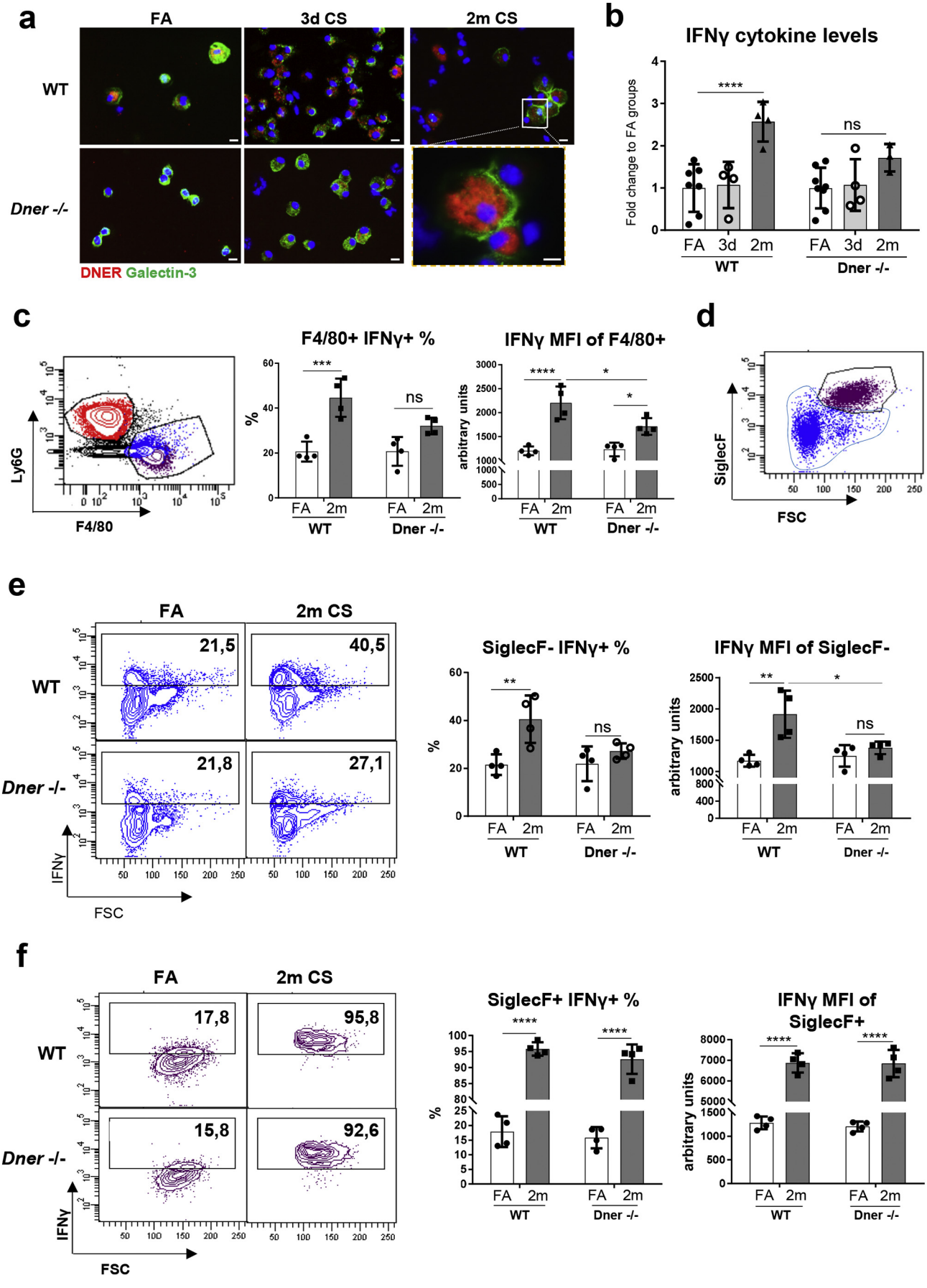
a
FA
3d CS
2m CS
WT
Dner -/-
DNER Galectin-3
b
IFNγ cytokine levels
Fold change to FA groups
****
ns
FA 3d 2m
WT
FA 3d 2m
Dner -/-
c
F4/80+ IFNγ+ %
IFNγ MFI of F4/80+
Ly6G
F4/80
%
arbitrary units
***
ns
****
*
*
FA 2m
WT
FA 2m
Dner -/-
d
SiglecF
FSC
e
FA
2m CS
WT
Dner -/-
21,5
40,5
21,8
27,1
IFNγ
FSC
SiglecF- IFNγ+ %
IFNγ MFI of SiglecF-
%
arbitrary units
**
ns
*
FA 2m
WT
FA 2m
Dner -/-
f
FA
2m CS
WT
Dner -/-
17,8
95,8
15,8
92,6
IFNγ
FSC
SiglecF+ IFNγ+ %
IFNγ MFI of SiglecF+
%
arbitrary units
****
FA 2m
WT
FA 2m
Dner -/-

difference in IFNγ secretion between both genotypes after CS exposure (Fig. 3f). Along similar lines, innate and adaptive immune populations after CS exposure were not altered in the lungs of DNER deficient mice compared to WT (Supplementary Fig. 3d, e). Thus, explaining the partial enhancement of total IFNγ levels in BAL from 2 month CS-exposed DNER deficient mice (Fig. 3b). Previous studies have shown that high levels of IFNγ leads to significant emphysema development [30]. Interestingly, 2 months CS exposed DNER deficient mice showed a significantly retained lung function, measured as FEV100, compared to CS exposed WT mice (Supplementary Fig. 3b). This was further supported by an absence of emphysema development in DNER deficient mice after 2 months CS exposure (Supplementary Fig. 3c). Taken together, these results revealed that DNER regulates IFNγ secretion in lung recruited macrophages and is crucial for CS-induced emphysema development.

3.4. DNER activates Notch1 signalling in response to CS

Several studies have shown that Notch-NFκB crosstalk signalling regulates IFNγ transcription [31,32]. To determine whether DNER deficiency affects Notch signalling in lung macrophages, we quantified the number of nuclear NICD1$^+$ Gal3$^+$ cells (white arrows, Fig. 4a) in lung sections from FA and 2 months CS-exposed mice. Interestingly, DNER deficient mice revealed significantly reduced nuclear translocation of NICD1 in macrophages after 2 months of CS exposure in comparison to WT mice (Fig. 4a-b). In support, the Notch1 signalling pathway was enriched in WT M1 compared to DNER deficient M1 macrophages (Fig. 4c, Supplementary Fig. 4a) and a similar pattern was observed in MDM from COPD patients (Fig. 4d). This could suggest that COPD macrophages have an altered Notch signature similar to the one observed in WT versus DNER deficient lung macrophages after CS exposure. Taken altogether, this data demonstrated that CS induced Notch1 activity in alveolar macrophages in vivo via DNER.

Further, to decipher whether DNER regulates IFNγ expression via Notch1-NFκB crosstalk, WT and DNER deficient BMDM were treated with LPS ex-vivo. First, we evaluated our previous results (Fig. 2e, f) by measuring IFNγ cytokine levels in the cell supernatants. As expected, IFNγ concentration after LPS stimulation was significantly reduced in the DNER deficient BMDM cell medium compared to the WT BMDM (Supplementary Fig. 4b). Upon LPS stimulation, DNER deficient BMDM showed reduced release of NICD1 to the cytoplasm and complete absence of NICD1 nuclear translocation in contrast to WT BMDM (Fig. 5a). *Notch1* expression was similarly increased after LPS treatment in both genotypes suggesting that reduced NICD1 in DNER deficient BMDM is not due to lower Notch1 receptor levels (Fig. 5b). Likewise, the gene expression of other Notch family members expressed in macrophages was not affected in the DNER deficient BMDM (Fig. 5b).

Consistent with this, we found that the quantification of NFκB subunits revealed that cytoplasmic levels of c-Rel, p105 and p50 were reduced in DNER deficient BMDM compared to WT before and after LPS treatment (Fig. 5c). Interestingly, there was no nuclear translocation of the NFκB subunits in DNER deficient BMDM with the exception of RelB, whose levels were reduced, compared to WT BMDM (Fig. 5c). This pronounced inhibition of the NFκB pathway was independent of IKKα/β activity, as its phosphorylation levels were unaltered (Fig. 5d). Together, this data clearly indicated that DNER is necessary for Notch activation and essential for nuclear activation of NFkB signalling after LPS treatment of pro-inflammatory macrophages. Transcriptomic analysis by GSEA and upstream regulator prediction using Ingenuity Pathway Analysis (IPA) supported this data. GSEA revealed enrichment of the NFκB downstream cascade in WT M1 compared to DNER deficient M1 BMDM (Fig. 5e and Supplementary Fig. 4c) and IPA predicted, with the lowest negative *Z*-score, the NFκB complex to be the most inhibited upstream regulator in DNER deficient M1 BMDM (Supplementary Fig. 4d). Taken all together, we have demonstrated that DNER is activating the Notch1-NFκB crosstalk pathway in BMDM after LPS activation.

4. Discussion

The absence of a curative therapy for COPD, make necessary the exploration of new targets. This is the first study that investigates the role of DNER, a novel non-canonical Notch ligand that appeared to be significantly associated with COPD patients in recent GWAS studies [19]. Here, we showed that *DNER* is upregulated in COPD human lung homogenates and localised to pro-inflammatory human and murine macrophages. In a CS-induced COPD mouse model, induced DNER expression is necessary for IFNγ production in lung recruited macrophages during chronic inflammation. This was further supported in vitro, where M1 polarised DNER deficient BMDM failed to induce *Ifng* transcription in response to pro-inflammatory stimulus due to an aberrant activation of Notch1-NFκB crosstalk.

In sections of COPD and healthy lung tissue, we observed that DNER is predominantly expressed by NOS2 positive macrophages and that its mRNA levels are induced in human primary macrophages after an inflammatory stimulus. This might lead to the debate of whether *DNER* upregulation is related to COPD or is a smoking effect. Nevertheless, the authors from the GWAS also presented evidence of a lack of association between DNER and distinct smoking phenotypes, concluding that the SNP is associated with declined lung function rather than smoking. These findings together with our results, suggest that the presence of the SNP entails susceptibility for *DNER* expression in COPD patients. Indeed, exploration of the SNP genomic region using the ENSEMBL database showed that the SNP is located in a methylation-sensitive histone site and 286 bp upstream to transcription factor binding motifs (data not shown). However, it should be considered that smoking drives inflammation in the lung, and this can lead to DNER induction as well [19], independently of the presence of the SNP. In contrast to a previous study showing a positive correlation between gender and DNER expression, we did not observe any gender nor age effect on DNER levels (Supplementary Fig. 1a-b). Additionally, the use of inhaled corticosteroids (ICS), a common immunosuppressive medicament for COPD patients, did not seem to affect lung DNER expression either (data not shown). These data suggest that the increased *DNER* expression in COPD lung homogenates is most likely due to an increase in pro-inflammatory macrophages. Supporting this idea, a very recent proteomic analysis of sputum from asthmatic patients showed that DNER was increased among 15 other markers implicated in macrophage-related inflammation [33].

The predominance and contribution of different macrophage subpopulations to the immunopathogenesis of COPD is unclear, especially given the complexity and diversity that entails the macrophage population [34,35]. Regarding origin, some studies suggest that lung resident macrophages have greater ability to phagocytose and secrete anti-inflammatory cytokines, meanwhile recruited macrophages tend to have a more pro-inflammatory phenotype. Indeed, it is believed that

Fig. 3. DNER regulates IFNγ secretion in lung recruited macrophages during CS-induced chronic inflammation. (a) Representative immunofluorescence images of bronchoalveolar lavage (BAL) cells obtained from filtered air (FA) and 3 day or 2 month CS-exposed WT and DNER deficient mice stained to detect DNER (red), Galectin-3 (green) and DAPI (blue) (n = 2–3 mice per group). (b) Total IFNγ levels quantified by ELISA in BAL from FA, 3 day and 2 month CS-exposed WT and DNER deficient mice (n = 4 mice per group). (c, d, e and f) Flow cytometric analysis of Ly6g$^-$ F4/80$^+$ macrophage populations from the whole lung of FA and 2 month CS-exposed WT and DNER deficient mice (n = 4 mice per group). (c) Percentage of IFNγ$^+$ cells gated from Ly6g$^-$ F4/80$^+$ macrophages and the MFI of IFNγ staining in the Ly6g$^-$ F4/80$^+$ population. (d) Gating strategy for Ly6g$^-$ F4/80$^+$ SiglecF$^+$ and SiglecF$^-$ populations. (e) Percentage of IFNγ$^+$ cells gated from SiglecF$^-$ Ly6g$^-$ F4/80$^+$ macrophages (blue from d) and the MFI of IFNγ staining in the SiglecF$^-$ Ly6g$^-$ F4/80$^+$ population. (f) Percentage of IFNγ$^+$ cells gated from SiglecF$^+$ Ly6g$^-$ F4/80$^+$ macrophages (burgundy population from d) and the MFI of IFNγ staining in the SiglecF$^+$ Ly6g$^-$ F4/80$^+$ population. Two-way ANOVA, Tukey's multiple comparisons test, $^*p < 0.05$, $^{**}p < 0.01$, $^{***}p < 0.001$, $^{****}p < 0.0001$. Each data point represents an individual mouse. Data shown mean values ± SD. (b-c, e-f).

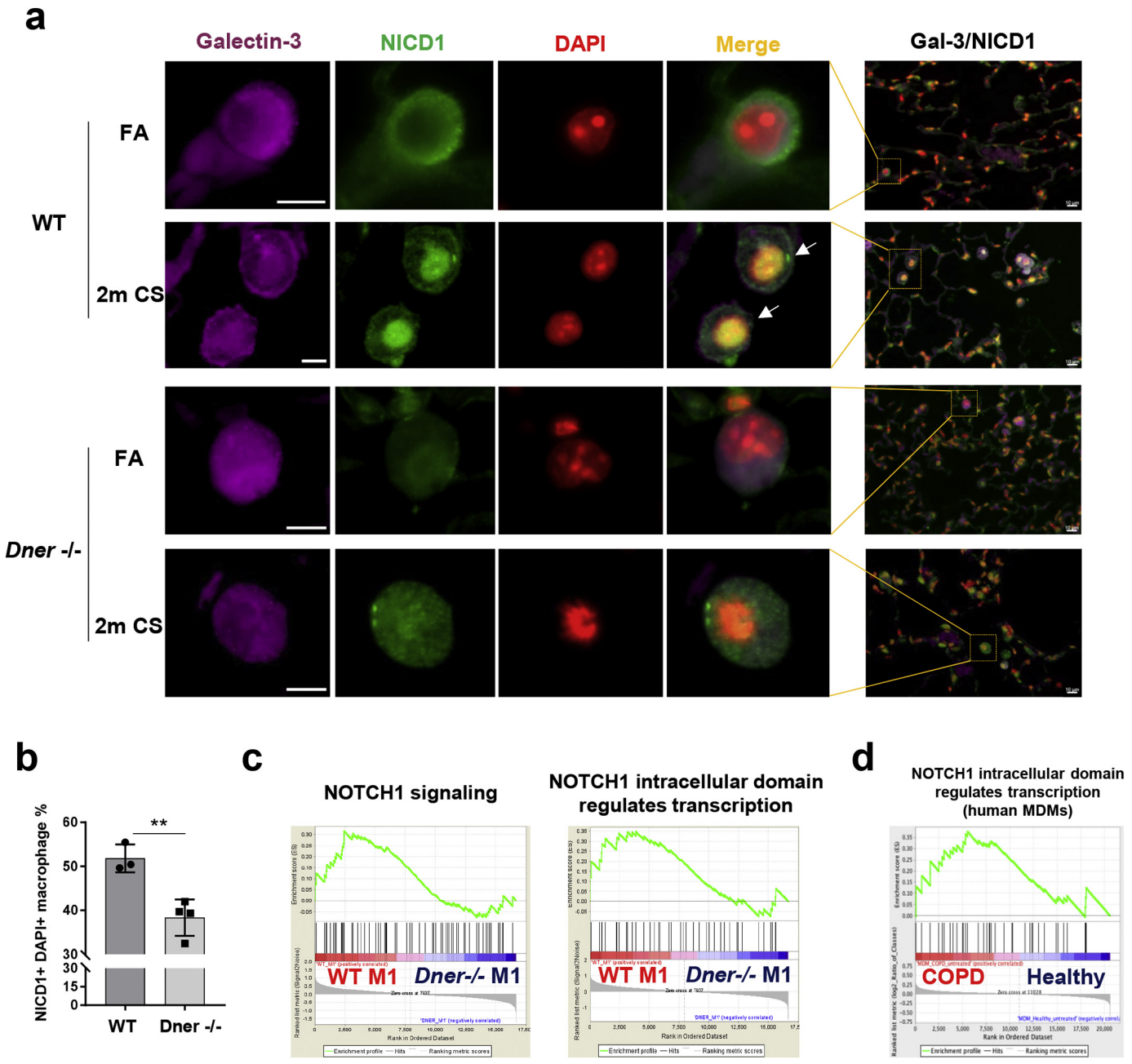

Fig. 4. DNER activates Notch1 signalling in alveolar macrophages from 2 month CS exposed mice. (a) Representative immunofluorescence images of lung tissue from FA and 2 m CS-exposed WT and DNER deficient mice (n = 3–4 mice per group), Galectin-3 (purple), NICD1 (green) and DAPI (red), high magnification, scale bars 5 μm; low magnification, 10 μm. Yellow squares indicate tissue location of the amplified macrophages. (b) Quantification of Galectin3^{+} cells showing NICD1^{+} DAPI overlap (white arrows shown in 4a) from staining in (a). 12 pictures at 20× magnification were taken from each mouse sample of each group. Unpaired t-test, $^{**}p$-value = 0.0055. No significant difference was found between FA groups. (c) Enrichment plots of Notch1 signalling from GSEA analysis of the microarray data from WT M1 vs DNER deficient M1 BMDM. (d) Enrichment plot of Notch1 signalling from the GSEA analysis of Monocyte Derived Macrophages (MDM) obtained from healthy and COPD patient microarray data (GSE8608).

when recruited macrophages enter the inflammatory zone, they become M1 in response to the ongoing insult, contributing to the exaggerated production of pro-inflammatory cytokines [10]. Concerning the macrophage phenotypes in the lung, recent reviews point to a direction of dysfunctionality in both phenotypes, M1 and M2, which results in defective cytokine secretion, migration and efferocytosis [14,15]. Nevertheless, it should be taken into account that the concept of M1/M2 emerged from an in vitro setting where the stimuli are known and stable [11]. Thus, it becomes controversial whether there is the existence of well-defined M1 and M2 subpopulations in a disease context, where the microenvironment constantly changes [10,34]. Together with the lack of appropriate markers to track these macrophage subpopulations, leads us to question whether in vitro findings can be extrapolated to what occurs during disease development. Nevertheless, we do believe that in vivo, a macrophage phenotype can be more pro than anti-inflammatory or vice-versa at a certain time and place, and this is what we would consider "M1" or "M2" in a disease context.

Several studies have shown that blockade of the Notch pathway improves disease resolution by regulating macrophage polarisation in autoimmune and inflammatory diseases [36,37]. Most of the published data consistently supports that Notch promotes a pro-inflammatory response in macrophages mainly by enhancing TLR and NFκB signalling [38,39]. Interestingly, our GSEA on monocyte derived macrophages (MDM) from COPD and healthy subjects showed an enrichment of the

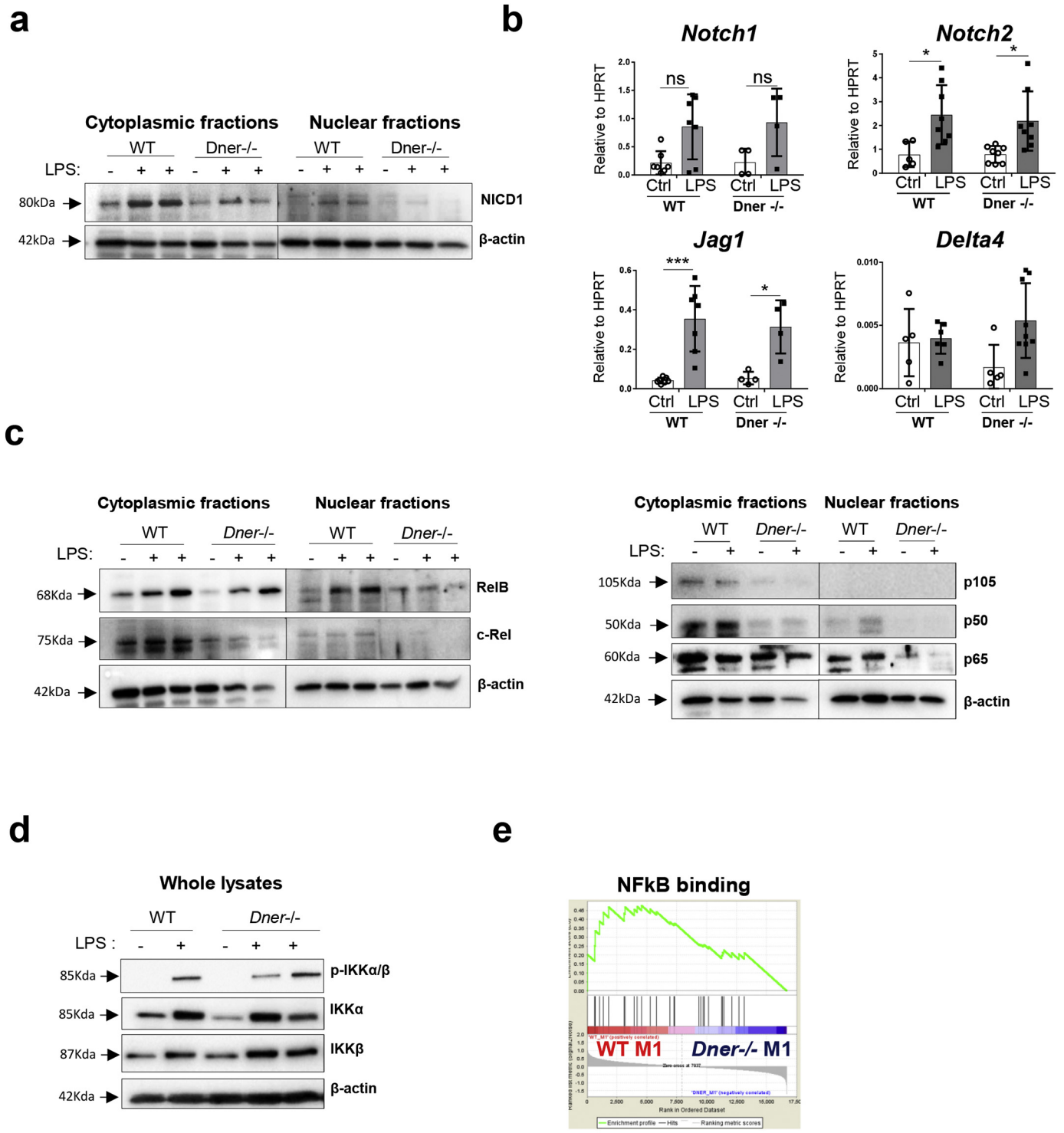

Fig. 5. Nuclear translocation of Notch1 and NFκB active subunits was abrogated in LPS treated BMDM from DNER deficient mice. (a) Representative Western blot of NICD1 protein levels in cytoplasmic and nuclear extracts of samples from WT and DNER deficient BMDM treated with LPS (1μg/ml) for 24 h and untreated (2 independent experiments, 2/3 biological replicates). (b) mRNA abundance of Notch receptors (*Notch1, Notch2*) and ligands (*Delta4, Jag1*) in the samples from (a). Two-way ANOVA, Tukey's multiple comparisons test, $^{*}P < 0.05$, $^{***}P < 0.001$. Data shown mean values ± SD. (c) Cytoplasmic and nuclear RelB, c-Rel, p105, p50 and p65 from samples described in (a). (d) Representative Western blots of phosphorylated (p)-IKKα/β, IKKα and IKKβ from 15 min LPS (1μg/ml) treated WT and DNER deficient BMDM. 2 independent experiments and 2/3 biological replicates, n = 3 (e) Enrichment plot of NFkB signalling (GO:0051059) following GSEA analysis of the microarray data from WT M1 vs DNER deficient M1 BMDM.

Notch pathway in COPD MDM. Here, we showed that DNER is essential for a fully functioning IFNγ driven M1 pro-inflammatory response in murine macrophages even though it was not crucial for delineating the distinct phenotypes.

IFNγ is one of the most upregulated cytokines in the lung of COPD patients [40,41]. Indeed, COPD MDM showed an enrichment of IFN pathways compared to healthy subjects. On the one hand, it plays a key role in promoting inflammation and tissue damage by polarising macrophages and T cells towards a type 1 response [29]. On the other, it induces bacterial clearance by activating phagocytosis and enhancing antigen presentation and nitric oxide production, important defence mechanisms during disease exacerbation [42,43]. Therefore, it should

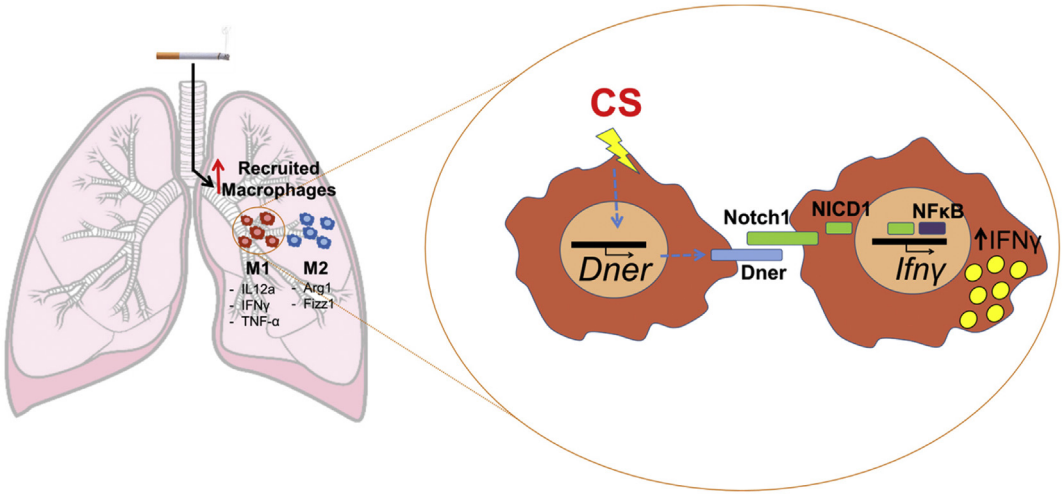

Fig. 6. Proposed role for DNER in macrophages during COPD inflammatory responses.

be considered that IFNγ may be beneficial as well as detrimental to the lung. Neutrophils, dendritic cells, NK, B, Th1 and $CD8^+$ T cells are all known to release IFNγ in response to infections and macrophage-driven inflammation [44,45]. Despite the fact that T cells are the most common IFNγ-producing cells [46], macrophages are the dominant cell population in a COPD lung [8], suggesting that macrophage contribution to IFNγ levels is likely considerable. Moreover, macrophages play a pivotal role in promoting inflammation at the early stage of disease, when IFNγ is involved [42,47,48]. Additionally, high levels of IFNγ can alleviate tissue injury by inducing TGFβ in macrophages [42] but it can also induce epithelial cell apoptosis and subsequent emphysema [30]. Thus, the precise regulation of IFNγ in COPD is essential to resolve infection without provoking an exaggerated inflammatory response. This would mean that dampening excessive levels of IFNγ, but not complete abrogation, could improve COPD patient outcomes. Here, we showed that IFNγ production is abrogated in recruited but not in resident macrophages from DNER deficient mice during chronic inflammation. In COPD, it has been suggested that recruited macrophages tend to acquire a pro-inflammatory phenotype, while resident macrophages become anti-inflammatory and pro-resolving cells [49]. Thus one could hypothesize that the blockage of DNER may modulate IFNγ levels and therefore control the exaggerated immune response in pro-inflammatory macrophages, without affecting the potential beneficial effects that IFNγ could exert in other cell types. Indeed, we showed that DNER deficiency in mice prevented CS induced emphysema and improved lung function (FEV100), without affecting the percentage or activation of the immune cell populations.

Currently, the molecular mechanism of non-canonical Notch signalling is controversial and poorly understood. It has been shown that DNER specifically interacts with the first and second EGF-like repeat of the extracellular domain of Notch1 by cell-cell contact, and activates gene transcription in a CSL-independent manner during Bergmann glia differentiation [21]. In this process, DNER cell location is precisely controlled by endocytosis to regulate its availability to interact with other neighbouring cells [50–52]. This explains why DNER, as a transmembrane protein, showed a cytoplasmic localisation in our immunofluorescence analysis. Indeed, previous analysis of DNER in neurons, showed a similar cellular distribution to the one we observe in macrophages [50,51].

Non-canonical Notch is characterized for being independent of CSL, and instead, regulating other signalling proteins such as the NFκB subunits [22]. Indeed, the presence of nuclear NICD1 is essential for NFκB signalling in T cells and macrophages to regulate transcription of pro-inflammatory cytokines. In Th1 cells, interaction of NICD1 with p50 and c-Rel regulates transcription of IFNγ in response to CD3/CD28 co-stimulation [31,32]. In the case of macrophages, it has been shown that NICD1 regulates nuclear translocation of NFκB subunits and it is able to directly bind to TNF and INOS promoters [39,53]. However, the Notch ligands upstream of these responses remains poorly understood. It has been suggested that Jag1 and Delta4 can trigger and maintain Notch signalling by the activation of a positive feedback loop in pro-inflammatory macrophages [54]. In order to undertake molecular studies to address the DNER induced signalling cascade in activated BMDM, macrophages were stimulated with LPS alone instead of the combination with IFNγ as performed for M1 polarisation, since IFNγ activates other pathways and a positive feedback loop [44], that could make it difficult to interpret the results. In contrast to previous studies, our data revealed that induced levels of Jag1 and Delta4 in LPS treated DNER deficient BMDM are not able to compensate for the reduction in IFNγ expression. Here, we showed that the non-canonical Notch ligand DNER regulates IFNγ transcription via NICD1 and NFκB signalling in primary murine macrophages upon LPS stimulation and in vivo chronic inflammation. Supporting these findings, quantification of triple nuclear $NICD1^+$ macrophages, revealed that DNER deficient 2 month CS-exposed mice exhibited reduced nuclear NICD1 translocation compared to WT macrophages which was accompanied by impaired nuclear translocation of the NFκB subunits in LPS stimulated BMDM from DNER deficient mice. In keeping with NFκB regulating the expression of the majority of cytokines in activated macrophages [55], gene levels of NFκB downstream targets, aside from IFNγ, was observed to be dampened in DNER deficient M1 macrophages as evidenced by GSEA and predictive upstream regulator analysis. Nevertheless, we would have expected a more pronounced reduction in cytokine expression given the strong abrogation of NFκB in LPS-treated DNER deficient BMDM. However, it should be taken into account that other key pathways for cytokine expression like MAPK cascade, ERK or JAK/STAT1 could partially compensate the absence of NFκB activation [56].

Taken all together, we speculate that exposure of lung recruited macrophages to the ongoing inflammatory insult during COPD progression, leads to increased levels of DNER and subsequent induction of IFNγ expression via a non-canonical Notch NFκB cross talk pathway in Notch1 positive macrophages (Fig. 6). This study not only adds new molecular insights to the complexity of Notch and the involvement of non-canonical signalling in COPD pathogenesis, but also opens new directions to further investigate novel targets for the treatment of COPD.

Author contributions

CBL and AÖY conceived the study and experimental design. CBL conducted the experiments. TMC contributed to FACS experiments, animal

preparation and GSEA analysis. ZE performed BMDM culture and cell fractioning. SEV provided the human samples. FG and IEF undertook experiments with human monocyte derived macrophages. MI and JB performed microarray analysis. CBL, TMC, OE and AÖY analysed and interpreted the data. CBL, TMC and AÖY wrote the manuscript. All authors read and edited the manuscript.

Declaration of interests

The authors declare no competing interests.

Acknowledgements

The authors acknowledge the technical assistance of Christine Hollauer (Helmholtz Zentrum München). We thank Dr. Stephanie J. London and Dr. Matthias Wjst for stimulating discussion. We gratefully acknowledge the provision of human biomaterial and clinical data from the CPC-M bioArchive and its partners at the Asklepios Biobank Gauting, the Klinikum der Universität München and the Ludwig-Maximilians-Universität München. This work was supported from the Helmholtz Alliance 'Aging and Metabolic Programming, AMPro' (J.B.). The funding bodies did not have any role in study design, data collection, data analysis, interpretation or writing of the report.

Appendix A. Supplementary data

Supplementary data to this article can be found online at https://doi.org/10.1016/j.ebiom.2019.03.054.

References

[1] Barnes PJ. Targeting cytokines to treat asthma and chronic obstructive pulmonary disease. Nat Rev Immunol 2018;1.
[2] Burney PG, Patel J, Newson R, Minelli C, Naghavi M. Global and regional trends in COPD mortality, 1990-2010. Eur Respir J 2015;45:1239–47.
[3] Barnes PJ. Cellular and molecular mechanisms of asthma and COPD. Clin Sci 2017; 131:1541–58.
[4] Jia J, Conlon TM, Sarker RS, Tasdemir D, Smirnova NF, Srivastava B, et al. Cholesterol metabolism promotes B-cell positioning during immune pathogenesis of chronic obstructive pulmonary disease. EMBO Mol Med 2018;10.
[5] John-Schuster G, Hager K, Conlon TM, Irmler M, Beckers J, Eickelberg O, et al. Cigarette smoke-induced iBALT mediates macrophage activation in a B cell-dependent manner in COPD. Am J Physiol Lung Cell Mol Physiol 2014;307:L692–706.
[6] Bhat TA, Panzica L, Kalathil SG, Thanavala Y. Immune dysfunction in patients with chronic obstructive pulmonary disease. Ann Am Thorac Soc 2015;12(Suppl. 2): S169–75.
[7] Barnes PJ. Immunology of asthma and chronic obstructive pulmonary disease. Nat Rev Immunol 2008;8:183–92.
[8] Finkelstein R, Fraser RS, Ghezzo H, Cosio MG. Alveolar inflammation and its relation to emphysema in smokers. Am J Respir Crit Care Med 1995;152:1666–72.
[9] Maeno T, Houghton AM, Quintero PA, Grumelli S, Owen CA, Shapiro SD. CD8+ T cells are required for inflammation and destruction in cigarette smoke-induced emphysema in mice. J Immunol 2007;178:8090–6.
[10] Yamasaki K, Eeden SFV. Lung macrophage phenotypes and functional responses: role in the pathogenesis of COPD. Int J Mol Sci 2018;19.
[11] Mills CD. Anatomy of a discovery: m1 and m2 macrophages. Front Immunol 2015;6: 212.
[12] Wang N, Liang H, Zen K. Molecular mechanisms that influence the macrophage m1-m2 polarization balance. Front Immunol 2014;5:614.
[13] Byrne AJ, Mathie SA, Gregory LG, Lloyd CM. Pulmonary macrophages: key players in the innate defence of the airways. Thorax 2015;70:1189–96.
[14] Kapellos TS, Bassler K, Aschenbrenner AC, Fujii W, Schultze JL. Dysregulated functions of lung macrophage populations in COPD. J Immunol Res 2018;2018:2349045.
[15] Vlahos R, Bozinovski S. Role of alveolar macrophages in chronic obstructive pulmonary disease. Front Immunol 2014;5:435.
[16] High M, Cho HY, Marzec J, Wiltshire T, Verhein KC, Caballero MT, et al. Determinants of host susceptibility to murine respiratory syncytial virus (RSV) disease identify a role for the innate immunity scavenger receptor MARCO gene in human infants. EBioMedicine 2016;11:73–84.
[17] Shaykhiev R, Krause A, Salit J, Strulovici-Barel Y, Harvey BG, O'Connor TP, et al. Smoking-dependent reprogramming of alveolar macrophage polarization: implication for pathogenesis of chronic obstructive pulmonary disease. J Immunol 2009; 183:2867–83.
[18] Walter W, Alonso-Herranz L, Trappetti V, Crespo I, Ibberson M, Cedenilla M, et al. Deciphering the dynamic transcriptional and post-transcriptional networks of macrophages in the healthy heart and after myocardial injury. Cell Rep 2018;23:622–36.
[19] Hancock DB, Soler Artigas M, Gharib SA, Henry A, Manichaikul A, Ramasamy A, et al. Genome-wide joint meta-analysis of SNP and SNP-by-smoking interaction identifies novel loci for pulmonary function. PLoS Genet 2012;8:e1003098.
[20] Busch R, Hobbs BD, Zhou J, Castaldi PJ, McGeachie MJ, Hardin ME, et al. Genetic association and risk scores in a chronic obstructive pulmonary disease meta-analysis of 16,707 subjects. Am J Respir Cell Mol Biol 2017;57:35–46.
[21] Eiraku M, Tohgo A, Ono K, Kaneko M, Fujishima K, Hirano T, et al. DNER acts as a neuron-specific notch ligand during Bergmann glial development. Nat Neurosci 2005;8:873–80.
[22] D'Souza B, Meloty-Kapella L, Weinmaster G. Canonical and non-canonical Notch ligands. Curr Top Develop Biol 2010;92:73–129.
[23] Eiraku M, Hirata Y, Takeshima H, Hirano T, Kengaku M. Delta/notch-like epidermal growth factor (EGF)-related receptor, a novel EGF-like repeat-containing protein targeted to dendrites of developing and adult central nervous system neurons. J Biol Chem 2002;277:25400–7.
[24] Tohgo A, Eiraku M, Miyazaki T, Miura E, Kawaguchi SY, Nishi M, et al. Impaired cerebellar functions in mutant mice lacking DNER. Mol Cell Neurosci 2006;31:326–33.
[25] Wang L, Wu Q, Zhu S, Li Z, Yuan J, Yu D, et al. Delta/notch-like epidermal growth factor-related receptor (DNER) orchestrates stemness and cancer progression in prostate cancer. Am J Transl Res 2017;9:5031–9.
[26] Sun P, Xia S, Lal B, Eberhart CG, Quinones-Hinojosa A, Maciaczyk J, et al. DNER, an epigenetically modulated gene, regulates glioblastoma-derived neurosphere cell differentiation and tumor propagation. Stem Cells 2009;27:1473–86.
[27] Tanabe N, Vasilescu DM, Kirby M, Coxson HO, Verleden SE, Vanaudenaerde BM, et al. Analysis of airway pathology in COPD using a combination of computed tomography, micro-computed tomography and histology. Eur Respir J 2018;51.
[28] Hofer TP, Frankenberger M, Mages J, Lang R, Meyer P, Hoffmann R, et al. Tissue-specific induction of ADAMTS2 in monocytes and macrophages by glucocorticoids. J Mol Med (Berl) 2008;86:323–32.
[29] Barnes PJ. Inflammatory mechanisms in patients with chronic obstructive pulmonary disease. J Allergy Clin Immunol 2016;138:16–27.
[30] Wang Z, Zheng T, Zhu Z, Homer RJ, Riese RJ, Chapman Jr HA, et al. Interferon gamma induction of pulmonary emphysema in the adult murine lung. J Exp Med 2000;192: 1587–600.
[31] Palaga T, Miele L, Golde TE, Osborne BA. TCR-mediated Notch signaling regulates proliferation and IFN-gamma production in peripheral T cells. J Immunol 2003; 171:3019–24.
[32] Shin HM, Minter LM, Cho OH, Gottipati S, Fauq AH, Golde TE, et al. Notch1 augments NF-kappaB activity by facilitating its nuclear retention. EMBO J 2006;25:129–38.
[33] Kasaian MT, Lee J, Brennan A, Danto SI, Black KE, Fitz L, et al. Proteomic analysis of serum and sputum analytes distinguishes controlled and poorly controlled asthmatics. Clin Exp Allergy 2018;48:814–24.
[34] Xue J, Schmidt SV, Sander J, Draffehn A, Krebs W, Quester I, et al. Transcriptome-based network analysis reveals a spectrum model of human macrophage activation. Immunity 2014;40:274–88.
[35] Franke-Ullmann G, Pfortner C, Walter P, Steinmuller C, Lohmann-Matthes ML, Kobzik L. Characterization of murine lung interstitial macrophages in comparison with alveolar macrophages in vitro. J Immunol 1996;157:3097–104.
[36] Zhang W, Xu W, Xiong S. Blockade of Notch1 signaling alleviates murine lupus via blunting macrophage activation and M2b polarization. J Immunol 2010;184:6465–78.
[37] Yin J, Hu H, Li X, Xue M, Cheng W, Wang Y, et al. Inhibition of Notch signaling pathway attenuates sympathetic hyperinnervation together with the augmentation of M2 macrophages in rats post-myocardial infarction. Am J Physiol Cell Physiol 2016;310:C41–53.
[38] Xu J, Chi F, Guo T, Punj V, Lee WN, French SW, et al. NOTCH reprograms mitochondrial metabolism for proinflammatory macrophage activation. J Clin Invest 2015; 125:1579–90.
[39] Monsalve E, Ruiz-Garcia A, Baladron V, Ruiz-Hidalgo MJ, Sanchez-Solana B, Rivero S, et al. Notch1 upregulates LPS-induced macrophage activation by increasing NF-kappaB activity. Eur J Immunol 2009;39:2556–70.
[40] Panzner P, Lafitte JJ, Tsicopoulos A, Hamid Q, Tulic MK. Marked up-regulation of T lymphocytes and expression of interleukin-9 in bronchial biopsies from patients with chronic bronchitis with obstruction. Chest 2003;124:1909–15.
[41] Reeves EP, Williamson M, Byrne B, Bergin DA, Smith SG, Greally P, et al. IL-8 dictates glycosaminoglycan binding and stability of IL-18 in cystic fibrosis. J Immunol 2010; 184:1642–52.
[42] Wang G, Lin A, Han Q, Zhao H, Tian Z, Zhang J. IFN-gamma protects from apoptotic neutrophil-mediated tissue injury during acute Listeria monocytogenes infection. Eur J Immunol Sep 2018;48(9):1470–80.
[43] Todisco T, Vecchiarelli A, Dottorini M, Eslami A, Bertotto A, Massucci M, et al. Interferon-gamma (r-IFN-gamma) induced activation of alveolar macrophages (AM) from anergic patients with chronic obstructive pulmonary disease (COPD). J Biol Regul Homeost Agents 1992;6:87–92.
[44] Hu X, Ivashkiv LB. Cross-regulation of signaling pathways by interferon-gamma: implications for immune responses and autoimmune diseases. Immunity 2009;31: 539–50.
[45] Wang G, Lin A, Han Q, Zhao H, Tian Z, Zhang J. IFN-gamma protects from apoptotic neutrophil-mediated tissue injury during acute listeria monocytogenes infection. Eur J Immunol 2018;48:1470–80.
[46] Schroder K, Hertzog PJ, Ravasi T, Hume DA. Interferon-gamma: an overview of signals, mechanisms and functions. J Leukoc Biol 2004;75:163–89.
[47] Sun K, Metzger DW. Inhibition of pulmonary antibacterial defense by interferon-gamma during recovery from influenza infection. Nat Med 2008;14:558–64.
[48] Wang F, Zhang S, Jeon R, Vuckovic I, Jiang X, Lerman A, et al. Interferon gamma induces reversible metabolic reprogramming of M1 macrophages to sustain cell viability and pro-inflammatory activity. EBioMedicine 2018;30:303–16.

[49] Aberdein JD, Cole J, Bewley MA, Marriott HM, Dockrell DH. Alveolar macrophages in pulmonary host defence the unrecognized role of apoptosis as a mechanism of intracellular bacterial killing. Clin Exp Immunol 2013;174:193–202.
[50] Fukazawa N, Yokoyama S, Eiraku M, Kengaku M, Maeda N. Receptor type protein tyrosine phosphatase zeta-pleiotrophin signaling controls endocytic trafficking of DNER that regulates neuritogenesis. Mol Cell Biol 2008;28:4494–506.
[51] Kurisu J, Fukuda T, Yokoyama S, Hirano T, Kengaku M. Polarized targeting of DNER into dendritic plasma membrane in hippocampal neurons depends on endocytosis. J Neurochem 2010;113:1598–610.
[52] Du J, Wang X, Zhang X, Zhang X, Jiang H. DNER modulates the length, polarity and synaptogenesis of spiral ganglion neurons via the Notch signaling pathway. Mol Med Rep 2018;17:2357–65.
[53] Boonyatecha N, Sangphech N, Wongchana W, Kueanjinda P, Palaga T. Involvement of Notch signaling pathway in regulating IL-12 expression via c-Rel in activated macrophages. Mol Immunol 2012;51:255–62.
[54] Palaga T, Wongchana W, Kueanjinda P. Notch Signaling in macrophages in the context of Cancer immunity. Front Immunol 2018;9:652.
[55] Hayden MS, West AP, Ghosh S. NF-kappaB and the immune response. Oncogene 2006;25:6758–80.
[56] Oeckinghaus A, Hayden MS, Ghosh S. Crosstalk in NF-kappaB signaling pathways. Nat Immunol 2011;12:695–708.
[57] John G, Kohse K, Orasche J, Reda A, Schnelle-Kreis J, Zimmermann R, et al. The composition of cigarette smoke determines inflammatory cell recruitment to the lung in COPD mouse models. Clin Sci 2014;126:207–21.
[58] Schneider CA, Rasband WS, Eliceiri KW. NIH image to ImageJ: 25 years of image analysis. Nat Methods 2012;9:671–5.
[59] Team RC. R: A Language and Environment for Statistical Computing; 2014.
[60] Subramanian A, Tamayo P, Mootha VK, Mukherjee S, Ebert BL, Gillette MA, et al. Gene set enrichment analysis: a knowledge-based approach for interpreting genome-wide expression profiles. Proc Natl Acad Sci U S A 2005;102:15545–50.